SMC-TR-98-28

AEROSPACE REPORT NO.
TR-96(8565)-7

A Model to Calculate Evaporative Oil Loss in Spacecraft Mechanisms

15 September 1998

Prepared by

D. J. CARRÉ and P. A. BERTRAND
Mechanics and Materials Technology Center
Technology Operations

Prepared for

SPACE AND MISSILE SYSTEMS CENTER
AIR FORCE MATERIEL COMMAND
2430 E. El Segundo Boulevard
Los Angeles Air Force Base, CA 90245

Engineering and Technology Group

THE AEROSPACE CORPORATION
El Segundo, California

REPORT DOCUMENTATION PAGE

Form Approved
OMB No. 0704-0188

1. AGENCY USE ONLY (*Leave blank*)	2. REPORT DATE	3. REPORT TYPE AND DATES COVERED
	15 September 1998	

4. TITLE AND SUBTITLE

A Model to Calculate Evaporative Oil Loss in Spacecraft Mechanisms

5. FUNDING NUMBERS

F04701-93-C-0094

6. AUTHOR(S)

Carré, David J., and Bertrand, Patricia Ann

7. PERFORMING ORGANIZATION NAME(S) AND ADDRESS(ES)

The Aerospace Corporation
Technology Operations
El Segundo, CA 90245-4691

8. PERFORMING ORGANIZATION REPORT NUMBER

TR-96(8565)-7

9. SPONSORING/MONITORING AGENCY NAME(S) AND ADDRESS(ES)

Space and Missile Systems Center
Air Force Materiel Command
2430 E. El Segundo Blvd.
Los Angeles Air Force Base, CA 90245

10. SPONSORING/MONITORING AGENCY REPORT NUMBER

SMC-TR-98-28

11. SUPPLEMENTARY NOTES

12a. DISTRIBUTION/AVAILABILITY STATEMENT

Approved for public release; distribution unlimited

12b. DISTRIBUTION CODE

13. ABSTRACT (*Maximum 200 words*)

Calculations of oil loss from ball bearings in space are generally limited by the oil vapor pressure data base used in the calculations. We have developed a computer model that ties oil loss behavior of linear hydrocarbons to empirical oil loss measurements. This results in more accurate determination of evaporative oil loss. Two oils are modeled. The application of the model for the oils to actual mechanisms is discussed.

14. SUBJECT TERMS

Evaporation
Lubricants
Mechanisms
Space Vehicles

15. NUMBER OF PAGES
24

16. PRICE CODE

17. SECURITY CLASSIFICATION OF REPORT	18. SECURITY CLASSIFICATION OF THIS PAGE	19. SECURITY CLASSIFICATION OF ABSTRACT	20. LIMITATION OF ABSTRACT
Unclassified	Unclassified	Unclassified	

NSN 7540-01-280-5500

Standard Form 298 (Rev. 2-89)
Prescribed by ANSI Std. Z39-18
298-102

Preface

The authors thank Mr. J. L. Childs for performing chromatography and oil loss measurements, Mrs. S. A. Jackson for oil loss measurements, and Mr. R. Bauer for the design and fabrication of the oil loss apparatus. In addition, the authors are grateful to Honeywell Satellite Systems Operation for permission to use their oil loss data.

Contents

Figures

Table

1. Introduction

To assess the rate of lubricant loss from a spacecraft mechanism and, thus, predict the lifetime of the mechanism under spacecraft environmental conditions, it is necessary to have a vapor pressure data base for the oils of interest under the temperature conditions of the application. Since petroleum-based oils are complex mixtures with a very large number of possible components, it is necessary to measure the weight loss as a function of time, temperature, and composition of the oil. This generally requires experimental capability and a large time investment.

In lieu of empirical measurements, vapor pressures of oils have been estimated by extrapolating high-temperature literature data for linear hydrocarbons (as representative of the oils) to the temperatures of interest. For this approach to be satisfactory, the following assumptions must be true: (1) the molecular weight vs component percent profile of the oil can be determined; (2) the physical properties of the chemical species in the oil are essentially the same as those for linear hydrocarbons; (3) the available literature high-temperature vapor pressure data for linear hydrocarbons are reasonably accurate; and (4) the Clausius-Clapeyron relationship is valid, i.e., a plot of log vapor pressure vs temperature is linear, or nearly so, for all the components in the oil. The Clausius-Clapeyron relationship is:

$$\ln P = \left(-\frac{\Delta H_{vap}}{RT}\right) + Const. \qquad (1)$$

where P is the vapor pressure in torr, H_{vap} is the enthalpy of vaporization in cal mol^{-1}, R is the gas constant in cal deg^{-1}mol^{-1}, and T is the absolute temperature in Kelvin. We have used the extrapolation approach in estimating the oil loss rates for a number of spacecraft mechanisms. We will show that our estimated vapor pressure values obtained by extrapolation were very conservative, through a comparison of empirically determined vapor pressure data from our laboratory. Vapor pressures are estimated from the high-temperature data, using a rigorous computer model for two commonly used oils. Also, we will show how the model can be used to predict evaporative oil loss in real systems.

2. Experimental

2.1 Materials

The two oils, OIL1 and OIL2, are petroleum-based oils obtained through the refining of crude oil. OIL1 is no longer produced. It is a highly refined mineral oil obtained from paraffinic base stock. OIL2 is refined from naphthenic oil base stock. Both oils are formulated with typical additive packages. Table 1 gives selected properties for the two oils.

Table 1. Selected Properties of Tested Oils

PROPERTY		OIL1	OIL2
Viscosity	cs, 40°C	27.4	98
	cs, 100°C	4.64	9.1
Viscosity Index		101	52
Pour Point, °C		-26	-9

2.2 Apparatus

The evaporation rates of the oils were measured using the apparatus shown in Fig. 1. It consists of 16 separate, removable aluminum cups that are each 1 cm internal diameter (sample surface area = 0.8 cm^2). The aluminum cups fit into holes in an aluminum base plate that is heated by a film heater. The temperature is measured and regulated using a thermocouple in the center of the base plate. The apparatus is housed in a bell jar that is evacuated using a turbomolecular pump. Background pressures were $<1 \times 10^{-3}$ Pa during the experiment, ensuring that free molecular flow conditions were maintained. The temperature of the oil in the sample cups was within 1°C of the sample holder during heating and during the test. The temperature at various positions in the holder was within 1°C of the regulated test temperature.

2.3 Procedure

Four ~50 mg samples of each oil were placed in four cleaned and preweighed (~ 1 g) aluminum cups. The cups were then weighed to determine the sample size to the nearest 0.01 mg. The samples ranged in mass between 50 and 55 mg. The oils formed smooth layers at the bottom of each cup, with only a small curvature at the cup edge. The cups were placed in the holes in the aluminum plate and installed in the bell jar. (The sample holder was preheated to the test temperature and was maintained at that temperature during all subsequent measurements to reduce the effects of apparatus heating time.) The system was then evacuated. The apparatus was maintained at the test temperature, 40°C, until a measurement was required. At that time, the system was vented with room air, and the sample cups were removed from the heated holder, cooled to room temperature, and weighed. The samples were then placed back in their original positions in the heated sample holder, and the bell jar was evacuated. This process was repeated to the end of the test. (At ambient pressure and temperature, evaporation is insignificant. The time under vacuum at the test temperature was used as the test time.)

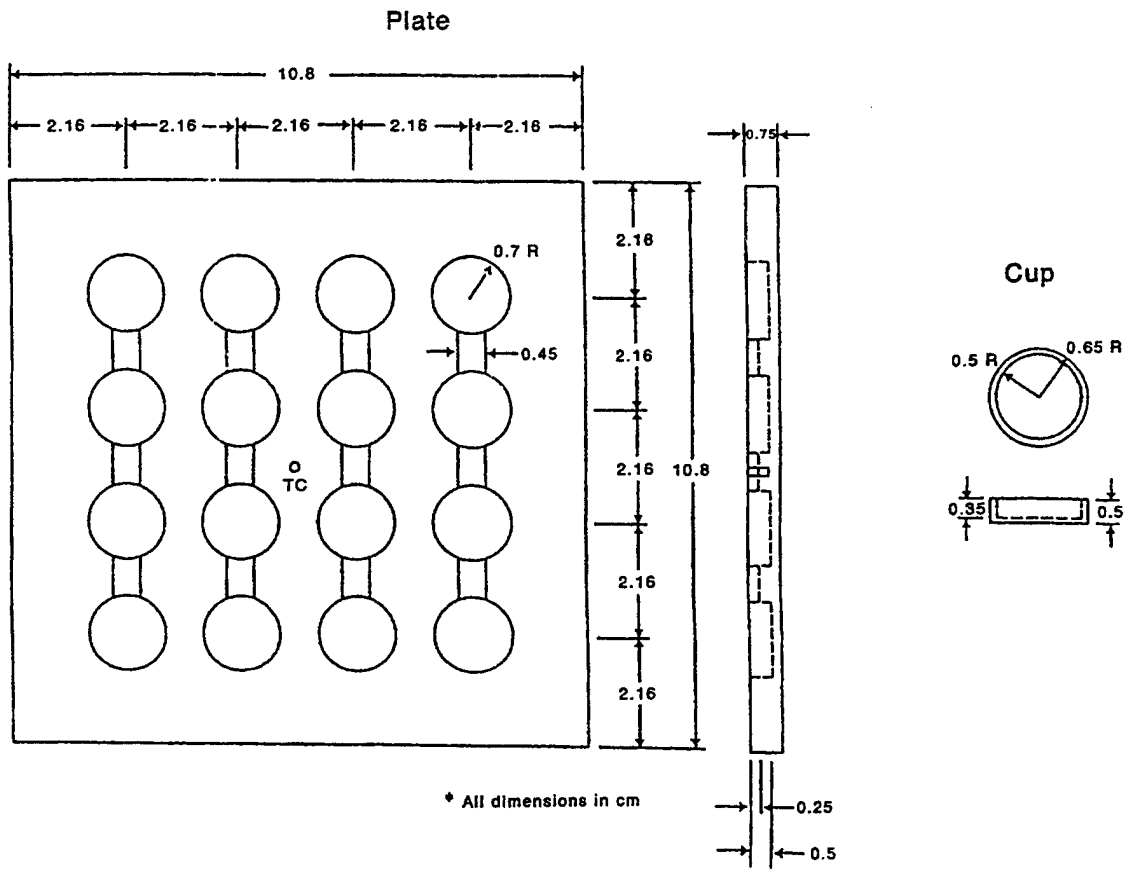

Figure 1. Oil evaporation apparatus.

3. The Model

Supercritical fluid chromatography (SFC) was used to estimate the molecular weight distribution of the two oils. The SFC uses a flame ionization detector that has a response that is proportional to mass. Linear hydrocarbon standards were run using SFC under the same conditions as the oils so that molecular weight vs retention time (the time each component resides on the chromatographic column) calibration could be determined. In SFC, compounds are eluted from the column as a function of their solubility in the supercritical carbon dioxide and their affinity for the coating on the inside of the column. For a homologous series of hydrocarbons (same structure, only changing in molecular weight) under the SFC parameters used, the retention time is proportional to molecular weight. Figures 2 and 3 give the SFC data, detector response vs retention time, for OIL1 and OIL2, respectively, and the linear hydrocarbon standards for the OIL1 conditions. Figure 4 shows a plot of retention time vs carbon number for five linear hydrocarbon standards run under the OIL1 SFC conditions as well as a least-squares fit to the data. Carbon number refers to the number of carbon atoms in the molecular formula for the hydrocarbon standards and is linearly related to the molecular weight and will be used as an "index" for the oil components. (A similar plot was obtained for the standards run under OIL2 SFC conditions but is not shown. Two different sets of SFC conditions were used for the two oils.) The least-squares fits are used to relate the SFC retention times to the carbon numbers of the oil components.

Computer files containing the SFC data (detector response vs retention time) for the two oils and the standards were converted to detector response vs carbon number as follows. Only the portions of the chromatograms in which the oils were being eluted were used. This is because the detector response to the solvent eluting at short retention times (not shown in the figures) dwarfs the other chromatographic features. For OIL1, 1300 data points at 0.02 min intervals, starting at approximately 13 min and ending at 39 min (Fig. 2), were used in the model. For OIL2, the data used in the analysis corresponded to 1232 points at 0.01667 min intervals (60 points/min), starting at approximately 15 min and ending at 35 min (Fig. 3). The effects of the "solvent tail" and the baseline were removed by subtracting the detector response due only to the solvent. This was accomplished by subtracting the data for the standards, with the peaks due to the standards removed from the trace and average baseline values substituted. This is especially important at short retention times that include the "tail" of the solvent detector response, as can be seen in Figs. 2 and 3. Using the equations for the least-squares fits of SFC retention time vs carbon number for the linear hydrocarbon standards, retention time was correlated with carbon number for each oil chromatogram.

The data can now be presented as detector response vs carbon number, with each data point at integer and noninteger carbon numbers representing an "oil component." Each of these "components" represents all the species that occur at that retention time (carbon number) in the oil for modeling purposes. The detector response is an integrated value for all these species. (Since there can be a large variation in structure and branching for the various species in the oil, the "component" carbon number is considered to be an average.) The baseline-corrected oil distribution as a function of carbon number for OIL1 is given as the 0% oil loss curves in Fig. 5. A similar plot can be obtained for OIL2 but is not shown.

Literature high-temperature vapor pressure data for 17 linear hydrocarbons *(1)* were fit to straight lines (log vapor pressure vs 1/T, the Clausius-Clapeyron relationship) using the least- squares method. Log vapor pressure values at 40°C were obtained by extrapolating the high- temperature data using the equation for the least-squares fit for each hydrocarbon. These extrapolated log vapor pressure data are presented vs carbon number in Fig. 6, as well as the least-squares fit to the

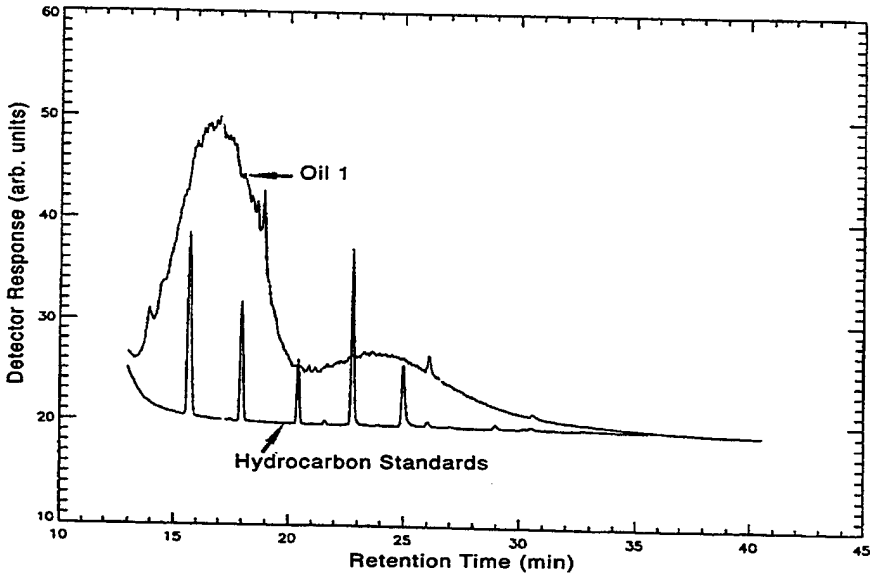

Figure 2. SFC chromatograms; OIL1 and hydrocarbon standards. The standards were not mixed quantitatively.

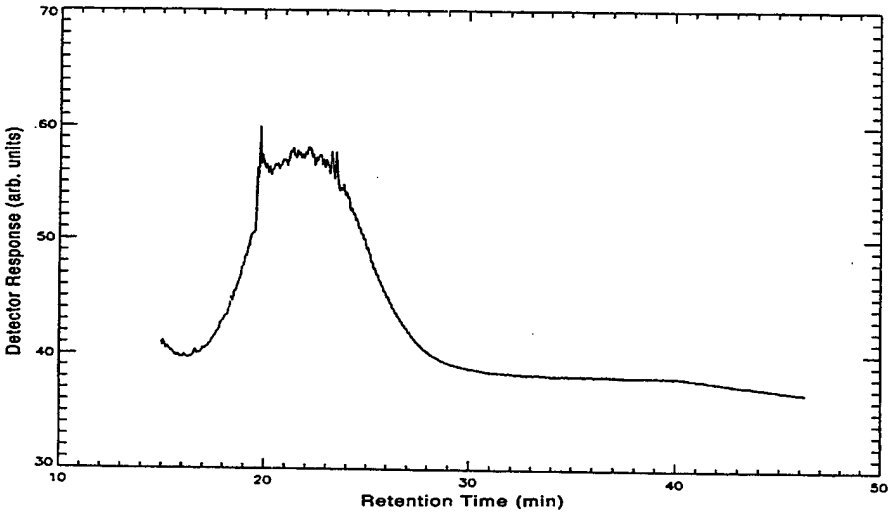

Figure 3. SFC chromatogram of OIL2.

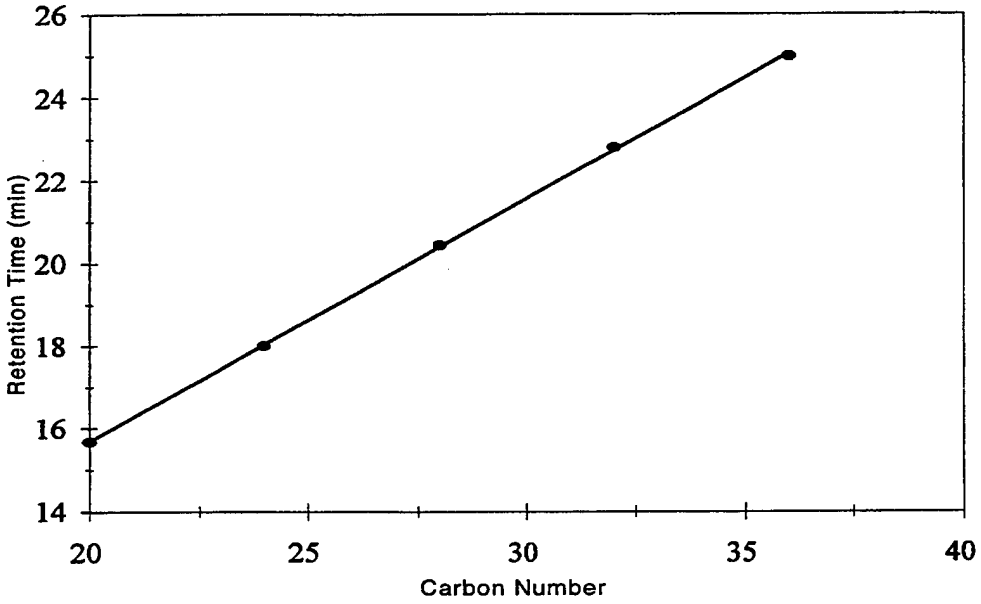

Figure 4. Retention time vs carbon number for hydrocarbon standards; OIL1 SFC conditions. (Carbon number refers to the number of carbon atoms in the molecular formula for the corresponding hydrocarbon standard.) Empirical data (●), least-squares fit (—).

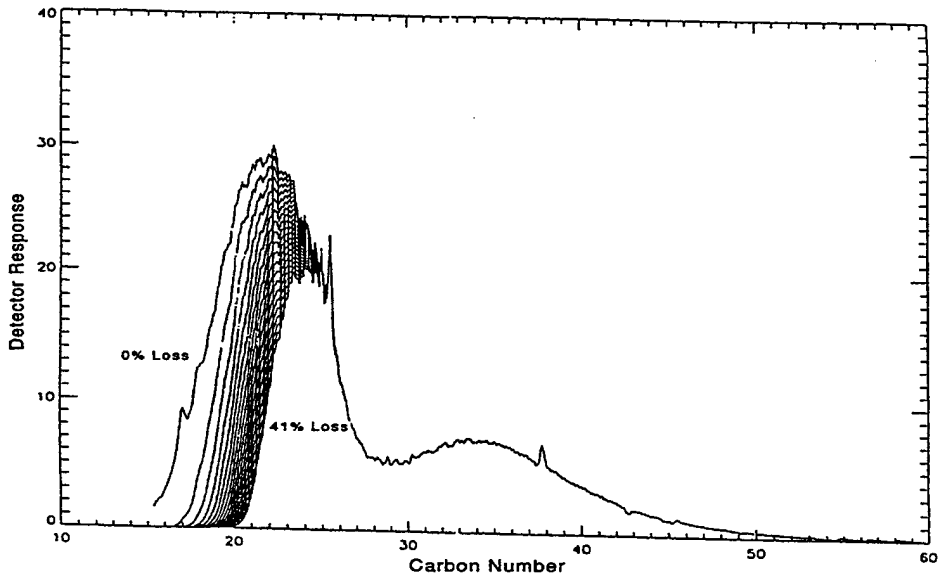

Figure 5. OIL1 component distribution with oil loss.

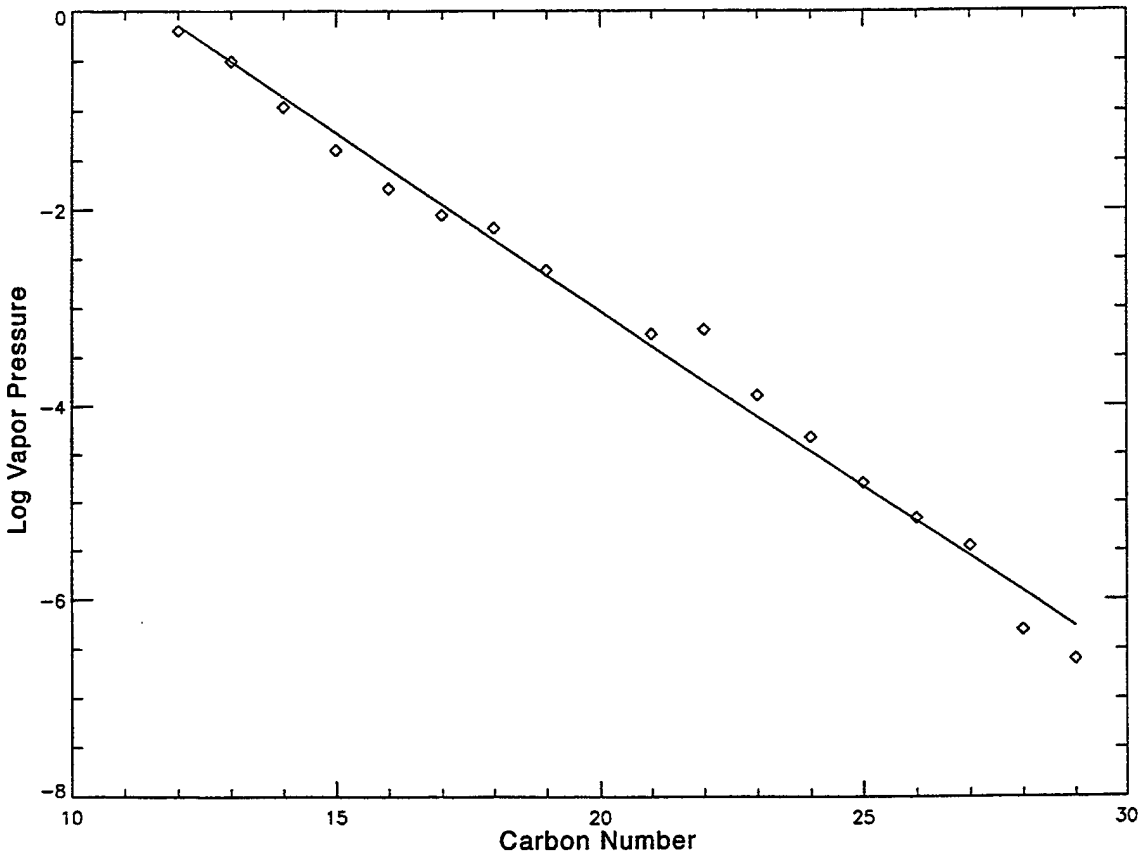

Figure 6. Log vapor pressure vs carbon number for linear hydrocarbon data extrapolated to 40°C; extrapolated data (◇), least-squares fit (—).

data. Using the equation for the least-squares fit, the vapor pressure for each "component" at 40°C could be computed for each oil (1300 and 1232 components for OIL1 and OIL2, respectively). The Langmuir equation,

$$P=17.14G\sqrt{\frac{T}{MW}} \qquad (2)$$

was used to calculate the mass loss rate for each component in each oil, where P is the vapor pressure in torr, T is the test temperature in Kelvin (313 K), MW is the molecular weight (obtained from the carbon number for each component), and G is the mass loss rate in g cm^{-2} s^{-1}.

A computer program was written in IDL® (Interactive Data Language) to calculate oil loss as a function of time. The inputs to the program are the detector response, the vapor pressure, the loss rate, the molecular weight, and the carbon number for each data point in the oil distribution. The SFC uses a flame ionization detector that has a response that is proportional to mass. Initially, in the program, the mass fraction and the mole fraction of each "component" are calculated. The initial total vapor pressure is calculated by summing the component partial pressures (Dalton's law) obtained by multiplying the vapor pressure of each component by its mole fraction (Raoult's law). The program contains an adjustable parameter whose value is chosen so that the extent of oil loss during a run can be selected. (This parameter represents a time step, times an area.)

The amount of loss of each component is determined by multiplying the component mass fraction times the loss rate for that component times the adjustable parameter. The amount of each component that has evaporated is subtracted from the previous oil distribution, and a new distribution is established. The mass and mole fractions, the total percent oil loss, and the total vapor pressure are calculated for the new distribution. Another "time interval" then occurs, resulting in a new oil distribution, mass and mole fractions, total percent oil loss, and total vapor pressure. The number of intervals that was used in this study was 500, although this number is also adjustable.

When the program is finished, the output consists of 500 total vapor pressures, total percent oil loss values, and oil distributions, corresponding to specific time intervals. Using these data, the vapor pressure as a function of oil loss can be plotted. In addition, the oil distribution at any of the time intervals can be plotted, generally as a function of carbon number. Figure 5 gives a representative plot of oil distribution vs carbon number. (Due to the large number of time intervals, distributions at every 25 time intervals are plotted.) Notice that there is greater loss between the early distributions than the later distributions and that the difference between distributions decreases with time. This is consistent with the fact that the lighter material is lost at a higher rate early in the evaporation process and the overall loss rate slows down with time.

4. Results and Discussion

The results of the laboratory oil loss measurements are shown in Figs. 7 and 8. In the figures, mass loss is plotted vs time for the two oils. The four OIL1 samples group nicely for the entire experiment. For OIL2, the values diverge somewhat at longer evaporation times. (Each sample is given a different symbol in the figures. A line representing the average of the data is included to guide the eye.) At the longer times, the change in mass is small. The divergence in the data is probably the result of the experimental error in handling, weighing the samples, and small differences in temperature due to sample position in the holder. The temperature variability is probably the largest factor, and could account for mass loss differences of several milligrams at the end of the experiment, due to evaporation rate differences for each cup. The precision of the weighing procedures is estimated to be ±0.1 mg.

In both the model and the analysis of the experimental data, we assume that the components of the oils are mixed rapidly via diffusion on the time scale of the evaporation experiments. We can check this assumption by calculating the total amount of the volatile fraction, M_t, that can be supplied to the surface in a given time interval, t, assuming that as soon as these molecules reach the surface, they evaporate. Then, if this calculated delivery amount is greater than the measured evaporated amount, the evaporation process is not limited by diffusion of volatile component from the bulk of the liquid to the surface. The supplied amount is *(2)*

$$M_t = 2C_o\sqrt{Dt/\pi} \tag{3}$$

where C_o is the initial concentration of the volatile fraction. D can be estimated as

$$D = \frac{RT}{6\pi\eta\sigma N_A} \tag{4}$$

where R is the gas constant (8.3 x 10^7 erg K^{-1} mol^{-1}), T is the temperature in Kelvin, η is the viscosity in poise, σ is the radius of the molecule in centimeters (about 10 Å), and N_A is Avogadro's number. D is about 1 x 10^{-7} cm^2 sec^{-1} for OIL1 and 3 x 10^{-8} cm^2 sec^{-1} for OIL2. Taking a 1 h time interval, we calculate M_t for OIL1 to be 7.3 mg cm^{-2} and M_t for OIL2 to be 2.4 mg cm^{-2}.

For OIL1 (see Fig. 7), the initial measured loss rate is 2.5 mg cm^{-2} h^{-1}, since the most volatile 20 mg of oil evaporates from a 0.8 cm^2 surface in 10 h. For OIL2 (see Fig. 8), the initial measured loss rate is 0.12 mg cm^{-2} h^{-1}, since the most volatile 10 mg of material leaves in 100 h. These evaporated amounts are much less than the amounts of material that could be supplied by diffusion from the bulk of the liquid, so the experiments are not diffusion limited.

The vapor pressure was calculated by determining the mass loss rate from the data, estimating the molecular weight for the fraction evaporating, and then using the Langmuir equation (eq. 2). The vapor pressure was then divided by 0.77, which is the appropriate Clausing conductance factor for the geometry of the evaporation cups *(3)*. The mass loss rate for each data point, the slope, was determined by using a three-point Lagrangian interpolation library subroutine in IDL. The slope values for the four sample sets for each oil were then averaged to get the average mass loss rate at

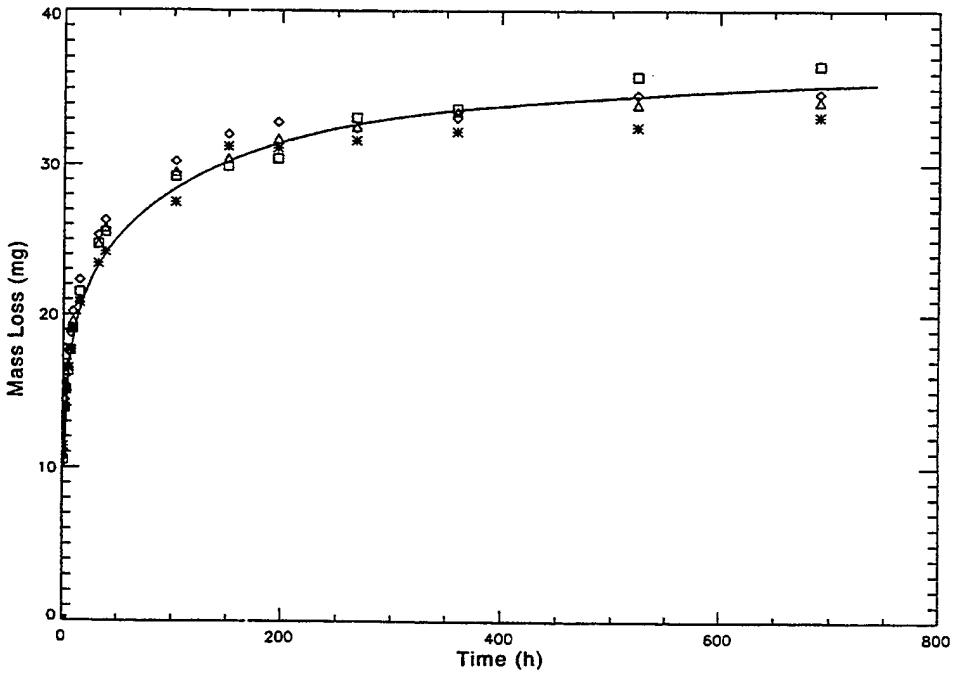

Figure 7. OIL1; mass loss vs time data. Measurement at 40°C.

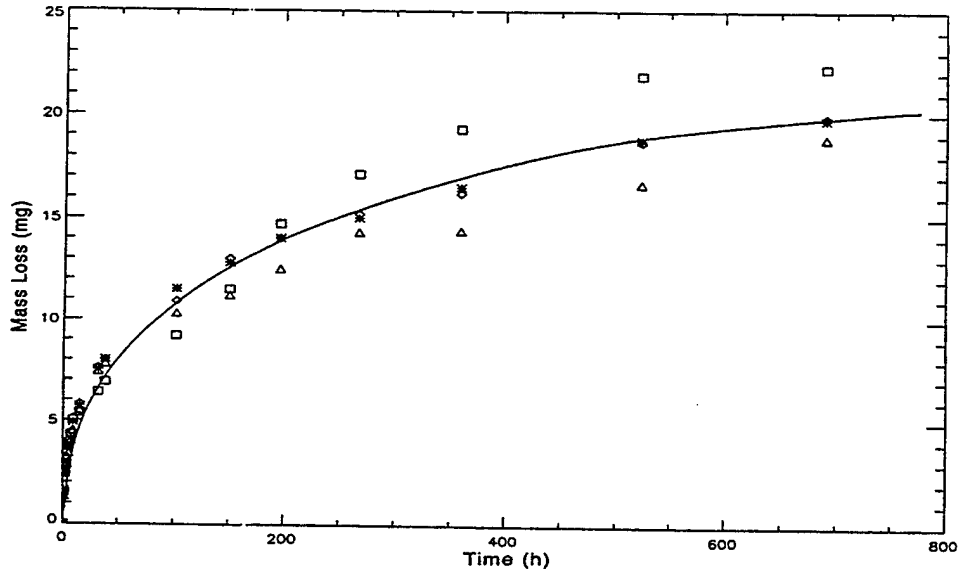

Figure 8. OIL2; mass loss vs time data. Measurement at 40°C.

each sampling time. We chose this approach because we felt it was more accurate than estimating the slope graphically from the mass loss vs time data. The percent oil loss for each oil was obtained by averaging the data for the four samples of each oil. From the oil distribution model data, a molecular weight was assigned to each percent oil loss value by taking the average molecular weight over 10 time intervals centered on the time interval that corresponded to the percent oil loss value of interest. (We do not actually know the average molecular weight of the oil being lost at each percent oil loss value. However, we did not feel that the approximation of the molecular weight using the model data would result in a significant error, since the square root of the molecular weight is used in the equation.)

Figure 9 gives the semilog plots of vapor pressure vs percent oil loss for the evaporation experiment (diamond symbols) and the model (solid line) for OIL1. The model results were obtained by piecing together several runs at different time intervals. At short time intervals, the 500 iterations resulted in low percent loss values at the end of the run. At large time intervals, so much is lost during the first time interval that the log vapor pressure vs percent oil loss curves are not smooth. Small mismatches occur at percent oil values where the segments are pieced together, such as approximately 15% oil loss in Fig. 9 and 45% oil loss in Fig. 10. However, these mismatches are small relative to the difference between the empirical and the model results. (This is also true for the OIL2 data to be discussed later.) For OIL1, the model data track the empirical data in shape, but the model vapor pressures are larger than the empirical vapor pressures by a factor of approximately 30. Except at low percentage oil loss values, both the model and the empirical data have nearly the same shape. The downward curvature in both the model and the test data is a reflection of the bimodal nature of the OIL1 distribution. Loss of the material in the first "hump" results in a large shift in the average molecular weight of the remaining material.

Figure 10 gives the semilog plots of vapor pressure vs percent oil loss for OIL2. As in Fig. 9, the diamond symbols represent the empirical data, and the solid line, the model. As was the case with OIL1, the empirical vapor pressure data for OIL2 are less than data predicted by the model, in this case, by a factor of approximately 100. Although similar in shape, there is a slight difference in the slopes between the model predictions and the empirical data.

The empirically determined vapor pressure as a function of oil loss is less than that predicted by the model, which is based on linear hydrocarbon, high-temperature vapor pressure data. The three possible explanations are (1) the original high-temperature data are not very accurate, (2) the log vapor pressure vs 1/T behavior of these materials is not linear over the large vapor pressure and temperature ranges over which the data are extrapolated, or (3) ΔH_{vap} is significantly different for linear hydrocarbons and the chemical species in the oils. The original data are from literature references for work done prior to 1900. It is possible that the techniques did not have a high degree of accuracy. Curvature in the Clausius-Clapeyron relationship would not be surprising, since it is known that curvature in plots of log vapor pressure vs 1/T occurs for a variety of compounds over ranges of temperature and vapor pressure that are considerably less than those used in the data extrapolations for the model *(4)*. In addition, estimates of changes in ΔH_{vap} using a group additivity approach are very large between room temperature and the boiling point for large hydrocarbons *(5)*. Thus, the curvature would be expected to be large enough to account for the differences between the experimental and model data. Unfortunately, we could not determine the curvature in the Clausius-Clapeyron plots using linear hydrocarbon standards, because the higher molecular weight species are solids at the lower temperatures of interest.

The similarity of shape of the plot of log vapor pressure vs percent oil loss between the model and the empirical data for oils may be the result of the similarity in molecular structure between the oil and linear hydrocarbons. OIL1 is a paraffinic oil, which implies that there is a significant

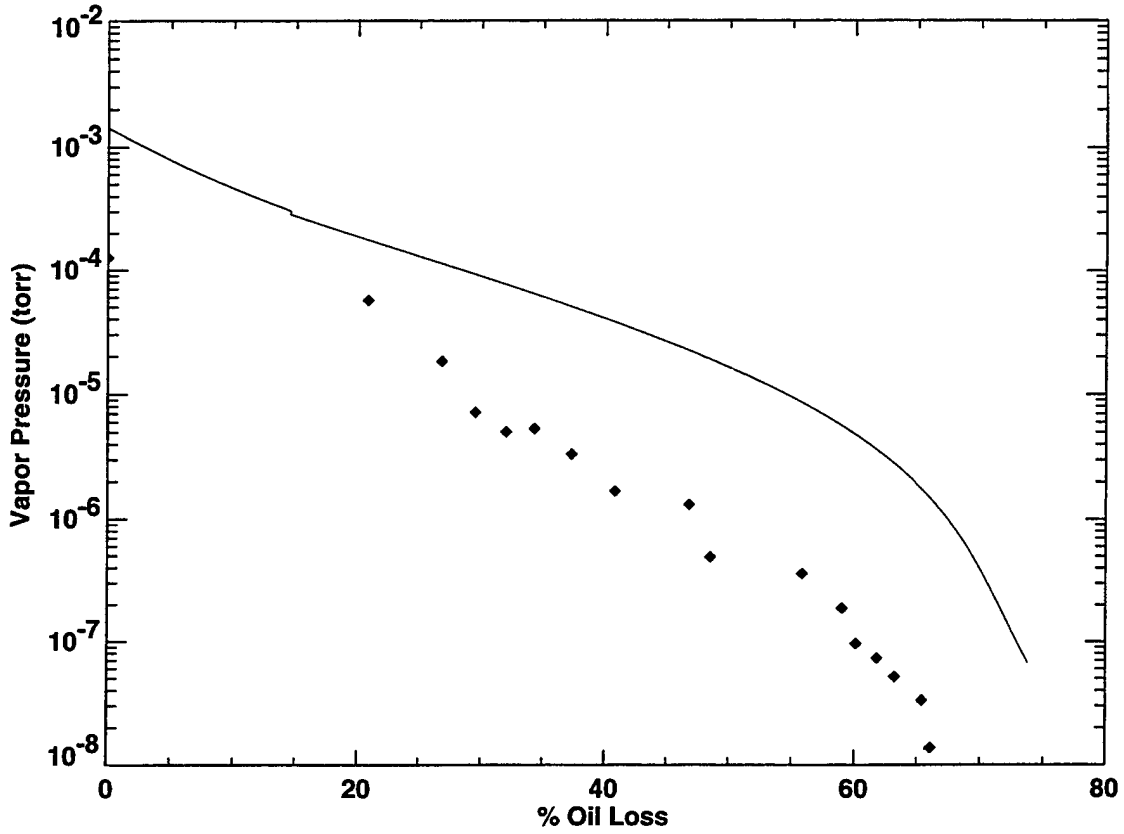

Figure 9. OIL1; vapor pressure vs % oil loss; model (—), empirical data (◆).

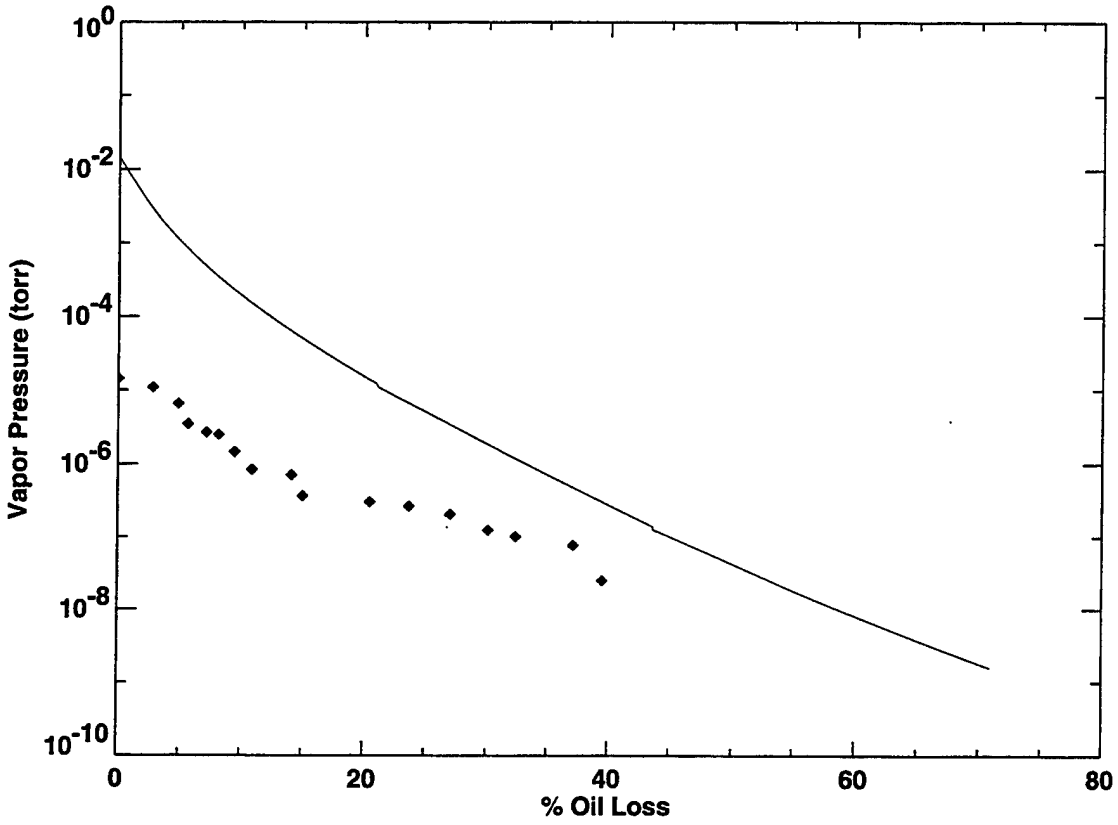

Figure 10. OIL2; vapor pressure vs % oil loss; model (—), empirical data (◆).

concentration of linear or moderately branched hydrocarbon components. On the other hand, the OIL2 data do not match quite as well. OIL2 is naphthenic and, thus, contains a large concentration of cyclic and highly branched species and thus is not expected to behave exactly like paraffinic hydrocarbons.

The validity of the model is illustrated in Fig. 11. SFC-derived oil distributions for OIL2 at 0% and 17.3% oil loss are shown, as well as the distribution provided by the model at 17.3% oil loss. The agreement is very good.

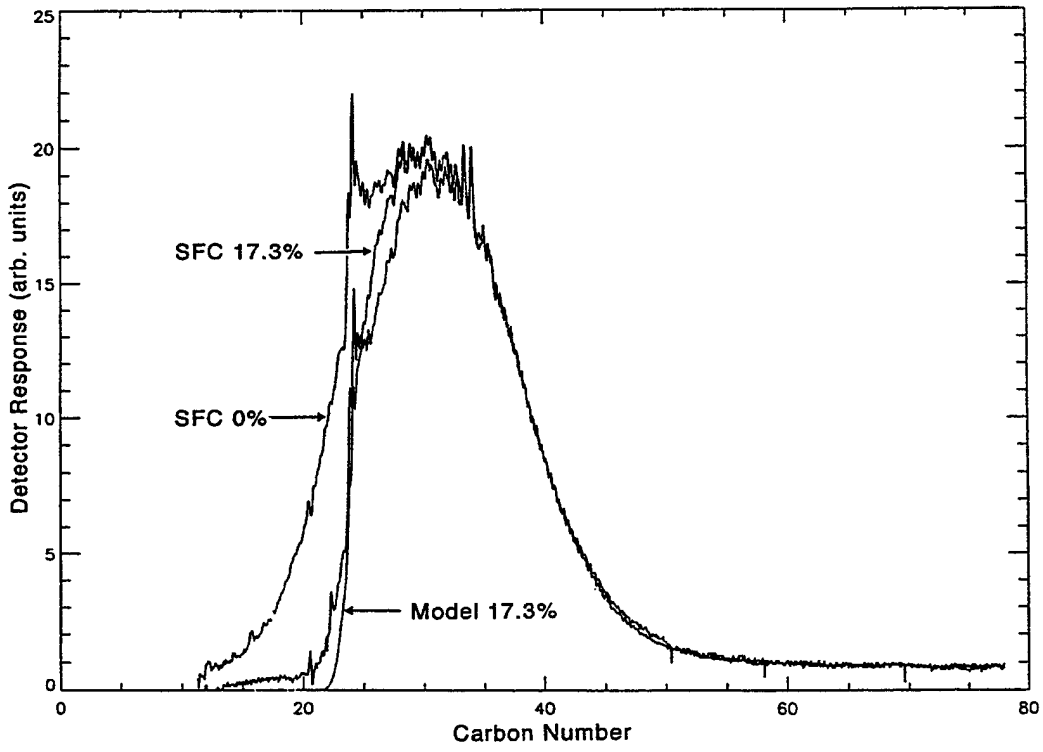

Figure 11. OIL1; comparison of model and empirical oil distributions at 17.3% oil loss.

5. Application of the Model

We present two examples in which the model results can be compared to actual oil loss data. We have approximated the effect of temperature on vapor pressure, the temperature factor, using ΔH_{vap} values calculated from the high-temperature linear hydrocarbon data. Using a least-squares fit, this leads to a relationship between temperature factor (TF) and carbon number (CN): TF = (CN*0.0854)+0.716, where TF for each component is defined as the value that the vapor pressure or loss rate must be multiplied by to accommodate each 10°C increase from the temperature, 40°C, for which there is empirical oil loss data. (Of course, for temperature less than that for the empirical data, the vapor pressures or loss rates would be divided by the TF.) We accept that this approximation may become inaccurate for very large molecules, but can be employed for hydrocarbon oils within the bounds of the following two assumptions: For most systems, oil loss will generally be less than 50%, which deemphasizes components larger than CN = 25; and, the temperatures modeled are ≤30°C from the temperature for which the empirical data are available. With the appropriate assumptions and limitations, the model can be used as a predictive tool. Since Trouton's rule implies that ΔH_{vap} is dependent upon boiling point and not structure at the boiling point temperatures, it would be of value to know the effect of structure on ΔH_{vap} at or near ambient temperature. However, since there are millions of components in a petroleum-based oil, we cannot know the structural characteristics of each component. Thus, although the question of the effect of structure and conformation on ΔH_{vap} is academically interesting, it is well beyond the scope of this paper and not germane to our model. The usefulness of the model depends upon how well it corresponds to actual oil loss. We are not interested in differences of 1% or 2% in oil loss; we are interested in determining whether oil loss will limit the lifetime of spacecraft systems.

The first example involves OIL2. Oil loss measurements were performed for a bearing cartridge system, under vacuum conditions at 70°C. There were no measurements before 65 h, and the test was terminated at 6% loss. The two data points at 100 h give an illustration of the possible errors in these measurements. The total amount of oil in the cartridge was 3.6 g. The loss rate from the cartridge is less than our open-pan experiments, because the cartridges are sealed with labyrinths that restrict the oil vapor flow. Using the standard labyrinth equations (*6*), the effective area of loss is 7.7×10^{-3} cm^2 for the cartridge. The results are given in Fig. 12. The symbols are the loss data, and the solid line is from the model. The model is within 1% of the empirical loss data.

The second example involves OIL1. During storage, the ball bearings in a satellite system suffered excessive lubricant loss. The system was stored under ambient temperature and with a background pressure of 0.5 atm of He gas. The evaporative oil loss was determined for five satellites stored 3, 5, and 7 years by comparing chromatographic data of the storage oil samples with that of unused oil. The loss was modeled using standard diffusion calculations and an average storage temperature of 25°C. The results are given in Fig. 13. As before, the symbols are the loss data, and the solid line is from the model. Only the storage portion of oil loss is shown. The small offset at 0 months is due to build and acceptance procedures. (These procedures were not performed on the cartridges in our first example.) Considering that the data point at 7 years is the least accurate, the correspondence between the model and the actual data is very good.

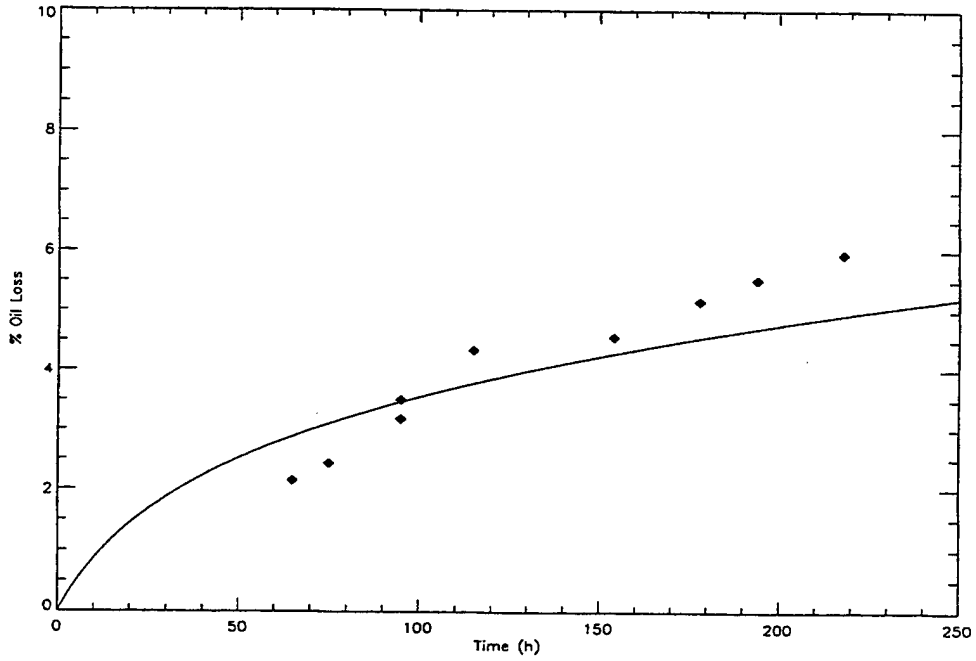

Figure 12. Comparison of model prediction and experimental bearing system 70°C oil loss data for OIL2; model (—), empirical data (◆).

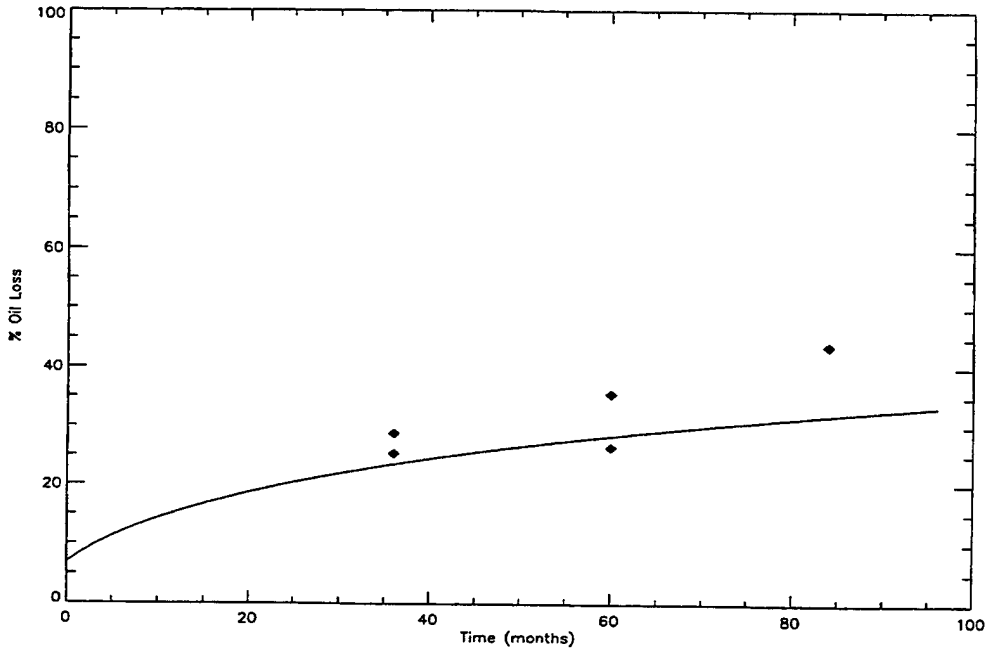

Figure 13. Comparison of model and empirical oil loss during satellite storage for OIL1; model (—), empirical data (◆).

6. Conclusions

The vapor pressures for two commonly used oils were determined empirically in our laboratory and predicted using a complex computer model. The model overpredicted the OIL1 and OIL2 vapor pressures by approximately factors of 30 and 100, respectively. This is due to extrapolation of high-temperature vapor pressure data to low temperature that does not account for curvature in the Clausius-Clapeyron relationship. Correcting the model vapor pressures using empirically determined loss data allows the model to be used to calculate lubricant loss. The model predictions were shown to compare favorably with actual oil loss data.

References

(1) Handbook of Chemistry and Physics, 49th ed., ed. R. C. Weast, The Chemical Rubber Co., Cleveland, OH, (1969).

(2) J. Crank, *The Mathematics of Diffusion*, Clarendon Press, Oxford, (1957).

(3) S. Dushman, *Scientific Foundations of Vacuum Technique,* second ed., John Wiley and Sons, New York, NY, (1962), p. 94

(4) F. Daniels and R. A. Alberty, *Physical Chemistry,* third ed., John Wiley and Sons, New York, NY, (1966), p. 127.

(5) N. Cohen and S. W. Benson, "The Thermochemistry of Alkanes and Cycloalkanes," in *The Chemistry of Alkanes and Cycloalkanes*, eds. S. Patai and Z. Rappoport, John Wiley and Sons, New York, NY, (1992), pp. 215-287.

(6) M. N. Gardos, "Labyrinth Sealing of Aerospace Mechanisms - Theory and Practice," *ASLE Trans., 17(4)*, 237-250 (1974).

TECHNOLOGY OPERATIONS

The Aerospace Corporation functions as an "architect-engineer" for national security programs, specializing in advanced military space systems. The Corporation's Technology Operations supports the effective and timely development and operation of national security systems through scientific research and the application of advanced technology. Vital to the success of the Corporation is the technical staff's wide-ranging expertise and its ability to stay abreast of new technological developments and program support issues associated with rapidly evolving space systems. Contributing capabilities are provided by these individual Technology Centers:

Electronics Technology Center: Microelectronics, VLSI reliability, failure analysis, solid-state device physics, compound semiconductors, radiation effects, infrared and CCD detector devices, Micro-Electro-Mechanical Systems (MEMS), and data storage and display technologies; lasers and electro-optics, solid state laser design, micro-optics, optical communications, and fiber optic sensors; atomic frequency standards, applied laser spectroscopy, laser chemistry, atmospheric propagation and beam control, LIDAR/LADAR remote sensing; solar cell and array testing and evaluation, battery electrochemistry, battery testing and evaluation.

Mechanics and Materials Technology Center: Evaluation and characterization of new materials: metals, alloys, ceramics, polymers and composites; development and analysis of advanced materials processing and deposition techniques; nondestructive evaluation, component failure analysis and reliability; fracture mechanics and stress corrosion; analysis and evaluation of materials at cryogenic and elevated temperatures; launch vehicle fluid mechanics, heat transfer and flight dynamics; aerothermodynamics; chemical and electric propulsion; environmental chemistry; combustion processes; spacecraft structural mechanics, space environment effects on materials, hardening and vulnerability assessment; contamination, thermal and structural control; lubrication and surface phenomena; microengineering technology and microinstrument development.

Space and Environment Technology Center: Magnetospheric, auroral and cosmic ray physics, wave-particle interactions, magnetospheric plasma waves; atmospheric and ionospheric physics, density and composition of the upper atmosphere, remote sensing, hyperspectral imagery; solar physics, infrared astronomy, infrared signature analysis; effects of solar activity, magnetic storms and nuclear explosions on the earth's atmosphere, ionosphere and magnetosphere; effects of electromagnetic and particulate radiations on space systems; component testing, space instrumentation; environmental monitoring, trace detection; atmospheric chemical reactions, atmospheric optics, light scattering, state-specific chemical reactions and radiative signatures of missile plumes, and sensor out-of-field-of-view rejection.